Hindawi Publishing Corporation
International Journal of Photoenergy
Volume 2012, Article ID 637839, 8 pages
doi:10.1155/2012/637839

Research Article

Acid Treatment of Titania Pastes to Create Scattering Layers in Dye-Sensitized Solar Cells

Trystan Watson, Cecile Charbonneau, Daniel Bryant, and David Worsley

SPECIFIC, College of Engineering, Baglan Bay Innovation and Knowledge Centre, Swansea University, Central Avenue, Baglan SA12 7AX, UK

Correspondence should be addressed to David Worsley, d.a.worsley@swansea.ac.uk

Received 3 August 2012; Accepted 28 September 2012

Academic Editor: Leonardo Palmisano

In dye-sensitized solar cells (DSC) scattering layers are used to increase the path length of light incident on the TiO_2 film. This is typically achieved by the deposition of an additional TiO_2 layer on top of an existing transparent film and designed to trap light. In this work we show that a simple acid pretreatment can lead to the formation of a scattering "skin" on the surface of a single TiO_2 film performing a similar function to a scattering layer without any additional depositions. This is important in increasing manufacturing throughput for DSCs as further TiO_2 depositions require additional materials and heat treatment. The pretreatment leads to self-assembly of a scattering layer of TiO_2 which covers the surface on short-term immersion (<30 min) and penetrates the bulk layer upon longer immersion. The method has been shown to increase the efficiency of the device by 20%.

1. Introduction

The development of the dye-sensitized solar cell (DSC) by Grätzel and coworkers [1–4] has drawn considerable attention due to its attractive combination of reasonable efficiency and low cost. Currently, there are a number of global industrialization projects aiming to take the DSC technology forward to the manufacture of larger area solar collectors based on roll-to-roll production methods [5]. Technologies have been developed to enable a viable manufacturing process route for DSC: faster sintering [6, 7] and dyeing [8] were advanced to address critical time-related process bottlenecks to the developing DSC manufacturing line. Another area driving manufacturing feasibility is the ability to combine or remove processes particularly in the energy intensive heating steps. Here we introduce a method for achieving a scattering layer effect in a single TiO_2 film without the need for bilayer film deposition and a second heating step.

The mesoporous TiO_2 film is perhaps the most important component in the multilayer DSC system. A number of treatments that can be carried out on the nanocrystalline TiO_2 layer have been proposed to enhance the performance of a DSC. These range from controlling porosity to polymer addition [9], modification of the TiO_2 by immersion in $TiCl_4$ [2, 4, 10] and by increasing the path length of incident light by the inclusion of scattering centres or layers [11, 12].

The scattering of light (and subsequent increase in optical path length) within TiO_2 films can be achieved by the inclusion of larger TiO_2 particles within the existing coating or the addition of a second or third coating containing larger particles on top of an existing transparent coating [4, 12–15]. The benefit of a multilayer system is well reported in terms of increasing light harvesting efficiency [15–18] with the additional films, containing larger TiO_2 particles, generating an optical confinement effect whereby light entering into the transparent working electrode is scattered by an opaque TiO_2 layer present on top of the original film.

Postsintering immersion of the TiO_2 film in acid has been proposed as a strategy for enhancing the efficiency of the device. A number of methods have been reported whereby the acid is used as a coadsorbant during the dyeing process [19], the consequent protonation of the TiO_2 film having been shown to facilitate the dye adsorption and suppress the back reaction of conduction band electrons to the tri-iodide

[20, 21]. The NO_3^- ions produced from HNO_3 immersion have also been suggested to coat the TiO_2 film and block the path of backward electron transfer [22]. In addition, acid enhancement has also been demonstrated by incorporating HCl into the TiO_2 powder during paste preparation [23] as a result of improvements to the dispersion of the nanoparticles.

In this paper we demonstrate the effect of presintering immersion of a single layer TiO_2 film in 2 M HNO_3. A presinter treatment leads to a time-dependant agglomeration of the TiO_2 inducing the formation of a scattering layer at the surface of the acid treated film on short-term immersion (<30 min) and penetrates the bulk layer upon long immersion. The advantage of this approach is that the TiO_2 paste can be applied in a single layer (i.e., one coating head or printing unit) and sintered once only. This new technique provides for considerable improvement of the TiO_2 film deposition process in terms of time and energy payback when compared to the traditional multilayer coating requiring either multiple coating heads and ovens or for material to be passed twice down a single-production line.

2. Experimental Details

2.1. Preparation of TiO_2 Photoelectrode. A commercial terpineol/ethyl cellulose based TiO_2 paste (DSL 18NRT, Dyesol) was deposited onto clean FTO (fluorine doped SnO_2 TEC 15, Solaronix) glass using a doctor blade technique. One layer of ~50 μm Scotch adhesive tape was used as a height guide. Following deposition the films were immediately placed into a bath of 2 M HNO_3 solution for varying times between 1 and 60 minutes at room temperature. On removal from the acid solution, the TiO_2 films were washed in doubly distilled water and allowed to dry for 5 minutes at room temperature before being placed directly into an oven for sintering at 450°C for 30 min. The process was purposely kept simple for the benefit of potential scale up by limiting the heat treatment to a single-sintering step. Reference TiO_2 photoelectrodes were prepared by water immersion for equivalent time periods followed by sintering (450°C for 30 min). The resulting films were characterized with a typical film thickness of ~7 μm. Upon cooling the films were sensitized by overnight immersion in a 0.3 mM dye (N719, Dyesol) solution, namely, cis-bis(isothiocyanato)bis(2,2′-bipyridyl-4,4′-dicarboxylato)-ruthenium(II) bis-tetrabutylammonium in a mixed acetonitrile/tert-butanol (1 : 1 v/v) solvent for 16–20 hours.

2.2. Optical and Microscopic Characterisation. Optical measurements were carried out on the TiO_2 deposited FTO glass after the nitric acid pretreatment and following sintering by recording the UV-Vis absorption spectrum of the TiO_2 films using a UV-Vis spectrophotometer (Lambda 750S, Perkin Elmer). The top surface and cross-section of the TiO_2 films were characterized by secondary electron imaging analyses on a S-4800 FEG-SEM apparatus from Hitachi (beam parameters: 1.5 keV, 10 μA, working distance: 3 mm). A clean cross-section of the TiO_2 film/glass substrate ensemble was obtained by forcing the sample to snap along a line prescored on the nonconductive side of the TCO substrate. Pore size distribution measurements were performed by nitrogen adsorption using a Tristar II 3020 from Micromeritics. In this case, the films were prepared onto microscope coverslips, which do not contribute to either porosity or surface area.

2.3. Photographic Method for Determining Dye Uptake. A Canon digital camera was used to record images of the front (glass side) and back (acid treated side) of the dye sensitized layers prior to cell assembly. The photographs were subjected to image analysis and the data was recorded in RGB format. In a separate study on dye uptake in opaque TiO_2 layers our dye uptake measurement method was shown to produce exactly the same overall information as measurements obtained by dye desorption combined with UV-Vis reflectance spectroscopy [24]. The ratio of the R (Red) value at the acid treated side/glass side (R_{back}/R_{front}) was further computed so that $R_{back}/R_{front} = 1$ is obtained for identical dye uptake throughout the TiO_2 layer, and $R_{back}/R_{front} < 1$ indicates a lower level of dye uptake on the acid treated face. This in house-developed characterization technique proved to be very convenient and rapid for assessing the differences in dye uptake either side of the TiO_2 layer, in a semiquantitative fashion. When compared to the more traditional dye desorption method, this new technique presents numerous advantages: it is much faster, considerably reduces the probability for experimental errors, is potentially applicable to a production line for quality control purposes, and makes it possible to discriminate between the dye uptake from both sides of the TiO_2 film (as opposed to quantifying the bulk amount of dye adsorbed throughout the entire thickness of the film).

2.4. Device Fabrication and Characterisation. Platinized counter electrodes were fabricated by deposition of a 5 mM solution of chloroplatinic acid (H_2PtCl_6, Sigma Aldrich) in IPA onto the FTO-coated glass, drying in air at T_{amb}, and immediate curing at 400°C for 30 min. Devices with 1 cm^2 active area were prepared by heat sealing the counter electrode to the TiO_2 film using 25 μm laser cut Surlyn (Meltonix 1170-25, Solaronix) gaskets. The electrolyte solution (0.8 M 1-propyl-3-methylimidazolium iodide (PMII), 0.3 M benzimidazole, 0.1 M I_2, and 0.05 M guanidinium thiocyanate dissolved in N-methoxy propionitrile) was introduced to the cell by vacuum injection through a single 0.5 mm diameter hole predrilled in the counter electrode (prior to platinization). The remaining hole was sealed by melting Surlyn through a circular microscope coverslip using a soldering iron. The current voltage characteristics of the cell were measured using a Sol3A solar simulator (94023A, Oriel), an AM1.5 filter and a Keithley 2400 source meter. A certified monocrystalline silicon reference cell (91150V, Oriel) traceable to the national renewable energy laboratory (NREL) was used to adjust the solar simulator to the standard light intensity of 1 sun, that is, 1000 W/m^2. The incident photo-to-current conversion efficiency (IPCE) of the dye-sensitized solar cells was measured with an IPCE system in the spectral range of 300–800 nm with a resolution of 5 nm.

3. Results and Discussion

3.1. Optical and Structural Properties of the Films. Upon immersion of the TiO_2 film into the acid solution a transition from transparent to opaque was immediately apparent. This striking phenomenon was seen to intensify with time, leading to complete opacity of the TiO_2 film within 30 minutes. Such observations are supported by the UV-Vis absorption spectra of films (after sintering) subjected to nitric acid treatment with increasing immersion time, as shown in Figure 1. An increase in the optical absorbance properties of the TiO_2 films in the visible range could be detected within 5 minutes of exposure to the acid solution; the absorbance of the TiO_2 films kept increasing up to 60 minutes although appeared visually opaque after 30 minutes. In comparison, immersion in water for over 1 hour did not seem to affect the degree of opacity of the TiO_2 film, its appearance remaining identical to films that were not immersed.

It should be noted that these measurements are made after sintering, meaning that the change induced during the dipping process is maintained after the binder has been removed and the particles sintered. The UV-Vis evidence is supported by FEG-SEM images shown in Figures 2 and 3, produced at varying intervals in the immersion process (also after sintering).

From the images presented in Figure 2, the application of the HNO_3 treatment appears to induce superficial porosity during the early stages (Figure 2(b)); this is followed by the progressive reorganization of the surface into a denser layer showing fewer and more elongated pores (Figure 2(c)); finally, a circular widening of the pores can be observed (Figure 2(d)). Overall these top view images show that immersion in a 2 M HNO_3 solution prior to sintering has altered the structure of the film at the surface in contact with the acid, causing the appearance of porous features responsible for the scattering of light and subsequent opacity of the films.

The time-dependant increase in opacity of the TiO_2 films can further be understood by looking at cross-section FEG-SEM images of the same films presented in Figure 3. After 5 minutes of immersion, the appearance of pores can be noticed at the superficial level of the film (Figure 3(a)) only, in correlation with previous observations (Figure 2(b)); Over time however the acid solution is able to penetrate the surface and induce progressive pore formation within the film, altering its structure over a depth of $\sim 2\,\mu$m within 20 minutes (Figure 2(c)); Eventually, a major transformation of the structure of the film, characterized with the formation of large aggregates throughout its entire thickness, is observed along with the reorganization of the surface into a very dense and thin (<50 nm) skin-like layer of TiO_2 (Figure 3(d)).

In summary, the time-dependant change in opacity of the TiO_2 films can be attributed to a progressive formation of larger pores initially at the surface exposed to the acid and then subsequently through the film, along with the formation of aggregates from the top to the bottom of the film for long-immersion times, and the reorganization of the surface of the film into a dense and thin skin-like layer. As these changes are induced by a presinter process it is likely

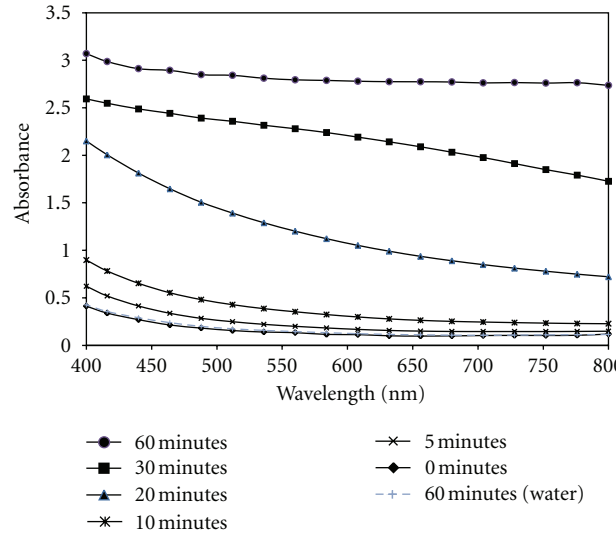

Figure 1: UV-Vis absorption spectra for nitric acid treated TiO_2 films with varying immersion times measured after sintering.

that the presence of the binder, in this case ethyl cellulose, plays in important role in the observed transformation. It is clear in Figure 1, that exposure to water has no effect, as such, acid additions are critical. We propose that the hydrolytic degradation of ethyl cellulose in the presence of nitric acid has a role to play in this phenomenon. We believe that the exposure of the paste to acid leads to the degradation of the cellulosic polymer chains releasing small volumes of water into the paste. The reorganization of the TiO_2 nanoparticle network would come about as a result of the generation of an essentially aqueous phase within the organic medium causing TiO_2 particles to be rejected from the organic matrix of the paste leading to the formation of aggregates of the type shown in the FEG-SEM images presented in Figure 3.

3.2. Effect of the Immersion Process on DSC Performance. Supporting evidence for agglomeration on the surface comes from the ability of the different surfaces (underside versus exposed side) to host the sensitizing dye. Typically, scattering layers are used for optical confinement purposes but considered inactive in terms of photon absorption; due to their low-surface area, scattering layer are characterized with low dye-uptake to the point of having visibly weaker coloration. Figure 4 presents the ratio of the R (red colouration) values obtained for the front (at the TCO glass/TiO_2 interface) and the back (at the nitric acid treated side of the TiO_2 film/air interface) of acid treated, sintered, and dyed TiO_2 layers. The R_{back} and R_{front} values were extracted from RGB values of photographs of the cells under identical lighting conditions. The data treatment here is semiquantitative, however, the analysis clearly shows the difference in dye uptake either side of the film in a way which could not be achieved by using the dye desorption method.

Figure 4 clearly shows a decrease of the R ratio over increasing immersion times, signifying that the dye uptake in the side of the film exposed to acid (shown

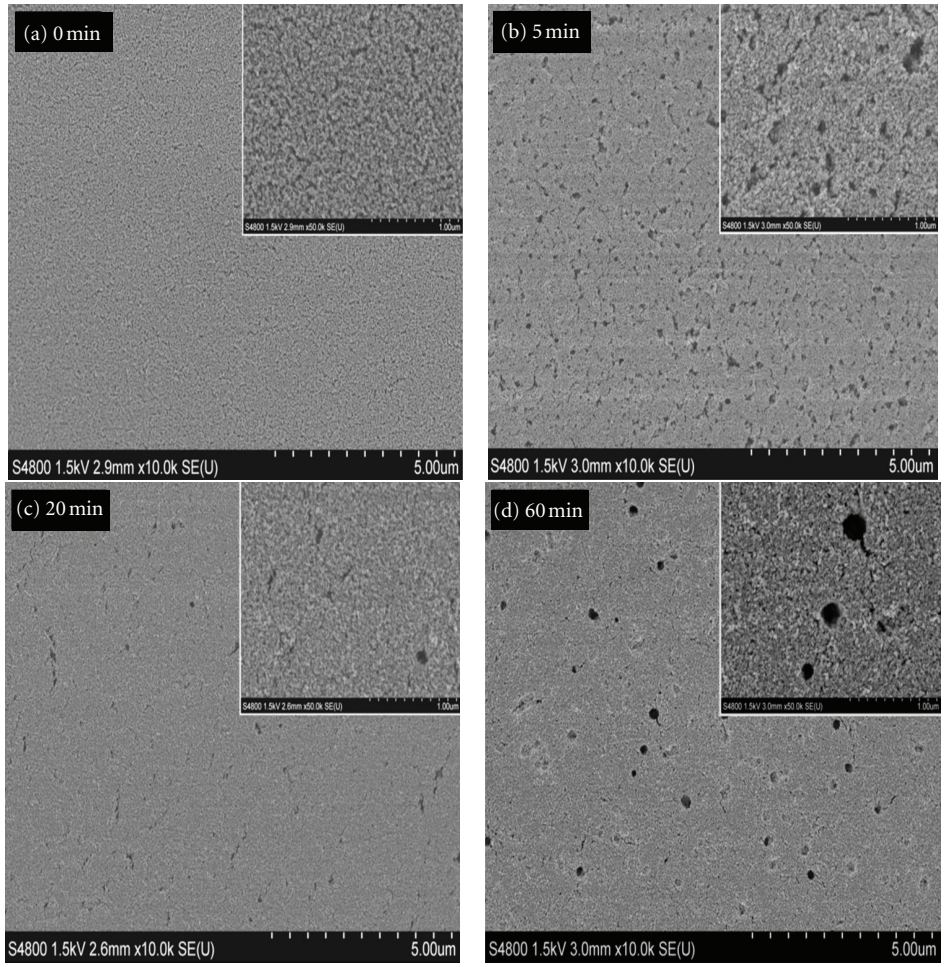

Figure 2: Top view FEG-SEM images (10 k mag. and 50 k mag. in the top right corner) of TiO_2 film (after sintering) submitted to nitric acid immersion for increasing amounts of time.

in Figures 2 and 3) decreases with acid exposure. Previous research has shown that aggregation of the particles in a TiO_2 film is potentially undesirable due to a reduced surface area [23], however the benefit of acid immersion is to restrict particulate aggregation to a single-exposed surface. Retaining modification to this surface layer is critical to developing the scattering effect while avoiding any unnecessary bulk aggregation and reduction in surface area for dye adsorption throughout the film as seen to occur beyond 20 minutes (Figure 3).

Porosity measurements were undertaken on films which were not exposed to acid and those exposed to acid for 60 minutes. This data is illustrated in Figure 5.

It can be seen the narrow pore size distribution characteristic of untreated TiO_2 films is lost upon 60 minutes exposure to 2 M HNO_3. Two clear features can be observed. Firstly, the pore size drops from ca 40 nm to around 10–15 nm on immersion in acid for 60 minutes. Since the dye itself typically has a size of ca 2 nm [25] this will result in poor dye uptake which aligns with the observations of lower coloration of the acid exposed face shown in Figure 4. In addition the data shows an expanded pore size at larger values (ca 200 nm) and above which correlates with the FEGSEM images and leads to the scattering effect.

Table 1 shows the photovoltaic characteristics of the TiO_2 films with varying immersion times following fabrication into 1 cm^2 DSCs. The efficiency can be seen to reach a maximum of 5.12% after 20 minutes of immersion—a 20% improvement on the nonimmersed sample. Whilst this initial data suggests 20 minutes is the optimum immersion period it is likely that the maximum effect is actually between 5 and 20 minutes. Further work is required to isolate the precise ideal conditions but it is clear that longer immersion is not effective. This is further illustrated in Figure 6, which presents a graphical representation of the DSC efficiency as a function of the immersion time. In parallel, the J_{sc} is seen to increase from 7.68 mA/cm^2 to 9.46 mA/cm^2 whereas the V_{oc} remains relatively unchanged, suggesting that the J_{sc} is responsible for the change in efficiency of the cells. This corresponds to the initial generation of uniform opacity across the wavelength range (Figure 1), and is consistent with the creation of a scattering layer (Figures 2 and 3). However, a prolonged immersion of the film effectively over ages this layer and limits the effect of acid enhancement:

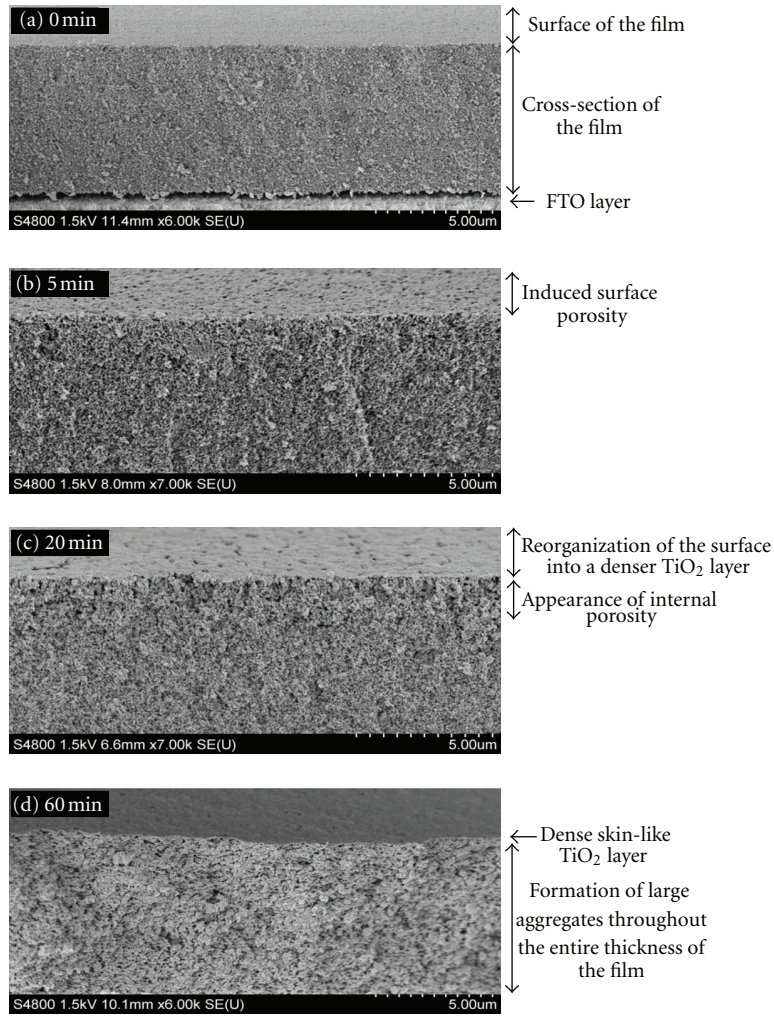

Figure 3: Cross section FEG-SEM images of TiO_2 film (after sintering) submitted to nitric acid immersion for increasing amounts of time.

intensification of the aggregation throughout the film over time leads to a reduction of the surface area available for dye adsorption, hence a decrease of J_{sc}. Immersion in distilled water over the same time period did not have an influence on the photovoltaic characteristics of the cell.

The way light is scattered through the TiO_2 film plays an important role in enhancing the light-harvesting effectiveness of the device and consequent incident photon-to-current conversion efficiency (IPCE). Figure 7 shows IPCE measurements of the cells produced after immersing the TiO_2 paste in 2 M nitric acid for different times prior to sintering and dyeing. The IPCE values can be seen to increase across the entire wavelength range with the immersion time, hence when the self-assembled scattering layer forms upon acid pretreatment. This is particularly noticeable for the area beyond 550 nm, a part of the spectrum where a conventional decrease in IPCE is usually ascribed to the low-absorption properties of N719 in the red region. This observation supports the view that the formation of a scattering layer is critical in improving the cell efficiency by enhancing the photon collection effectiveness of the film, even when lower dye uptake in achieved at the top of the film (Figure 4), here on the acid treated face.

In an attempt to further evaluate the effectiveness of the nitric acid pretreatment, the immersion of TiO_2 films was repeated in other acidic aqueous media, such as sulphuric, hydrochloric, and phosphoric acid with equivalent concentration (2 M). In this part of the study, a set immersion time of 20 min was adopted. All the films (including those treated with H_3PO_4) displayed an increase in opacity regardless of the acid type used, in an analogous fashion to that observed when using HNO_3. However, the results showed that HNO_3 outperforms the other acid types in terms of DSC efficiency improvements. In particular, the H_3PO_4-treated film generated virtually no current, which is related to the fact that the TiO_2 film (after H_3PO_4 treatment and sintering) visually did not adsorb any of the dye from solution. The performance of other acidic aqueous media are shown graphically in Figure 8.

This proves that not only the acidic and aqueous nature of the dipping medium, but also that the type of counter

Table 1: Performance characteristics of DSC under 1 sun of illumination based on a variation of acid immersion time. The active cell area is 1 cm^2 and 5 cells were produced for each data point.

Acid immersion time	V_{oc} (V)	J_{sc} (mA/cm^2)	FF	Efficiency (%)
0 min	0.73 (0.01)	7.68 (0.46)	0.74 (0.01)	4.15 (0.20)
1 min	0.72 (0.01)	8.20 (0.59)	0.71 (0.02)	4.17 (0.21)
5 min	0.75 (0.01)	9.46 (0.33)	0.71 (0.03)	4.98 (0.24)
20 min	0.72 (0.02)	9.91 (0.63)	0.72 (0.02)	5.12 (0.34)
60 min	0.73 (0.01)	9.80 (0.15)	0.72 (0.01)	5.09 (0.13)

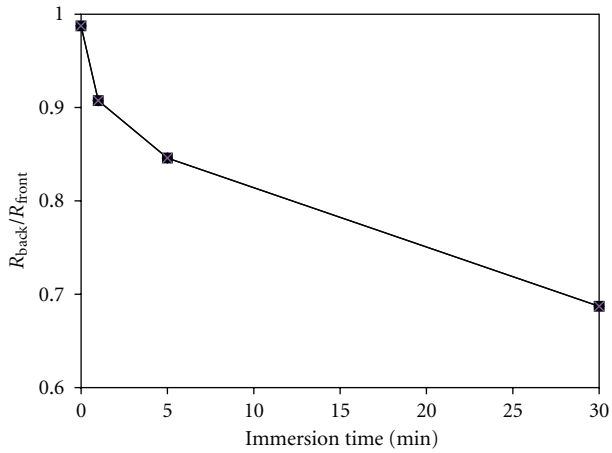

Figure 4: Ratio of R_{back}/R_{front} (R = red from RGB analysis) for dyed TiO_2 layers where the back face has been treated in 2 M HNO_3 for different immersion times. A value of 1 indicates identical colouration on both sides of the cell and values less than 1 indicate that less dye uptake is present on the acid-treated face.

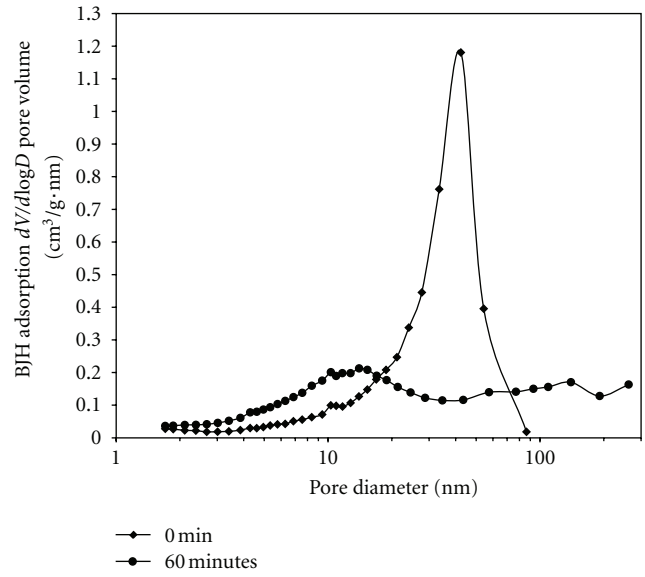

Figure 5: BJH adsorption pore size distribution measurements performed on untreated-TiO_2 films and films treated for 60 minutes.

anion is critical to inducing the desired scattering properties to TiO_2 photoanodes. When immersed in an acidic aqueous solution, TiO_2 particles become positively charged. The affinity of anions for positively charged surfaces, hence their potential to adsorb at the surface of the TiO_2 nanoparticles mostly depends on their electronegativity, which in order of magnitude in the case of nitrate, chloride, sulphate, and phosphate anions is ordered as follows: $\chi_{Phosphate} > \chi_{Sulfate} > \chi_{Chloride} > \chi_{Nitrate}$. From these observations, it may be assumed during the dipping process that anions adsorb at the surface of TiO_2 nanoparticles, in quantities related to their specific adsorption properties, where sufficient energy is provided during sintering to remove weakly bonded anions such as nitrates, it may not be sufficient to get rid of phosphate or sulphate ions, which are more strongly bonded to the surface of TiO_2 nanoparticles, resulting in a blockage of sites necessary for the subsequent adsorption of the dye. Further work is underway using a variety of commercial and lab prepared TiO_2 pastes varying acid type and strength, temperature, immersion time, and solution agitation to determine the wider application of the acid activation step in DSC paste activation.

4. Conclusions

An increase in power conversion efficiency by almost 20% is achieved by treatment of the TiO_2 photoelectrode with 2 M nitric acid prior to sintering. The efficiency increase is mirrored by a transition from transparent to opaque which relates to changes at the surface and gradually through the internal structure the TiO_2 film. An optimum immersion time for the system as described has been determined at 20 minutes at room temperature and is consistent with the development of pores along with the aggregation of TiO_2 nanoparticles within a layer of 2 μm thickness close to the acid exposed surface. These features are responsible for inducing scattering properties to the face in direct contact with the acid solution and improving light harvesting capabilities of the assembled cells. Longer term acid exposure leads to greater aggregation of TiO_2 within the photoelectrode which impacts negatively on cell performance by

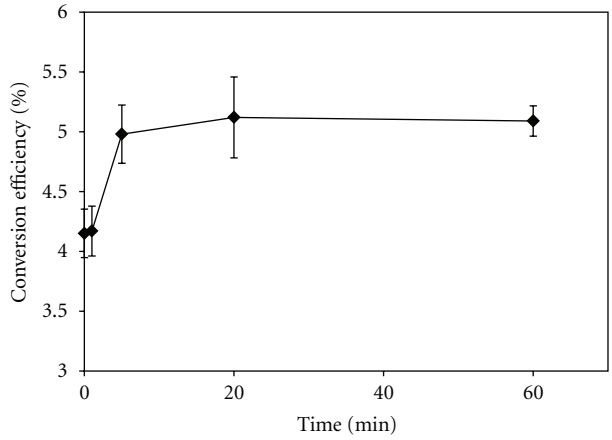

Figure 6: Influence of immersion time of TiO_2 films in nitric acid on power conversion.

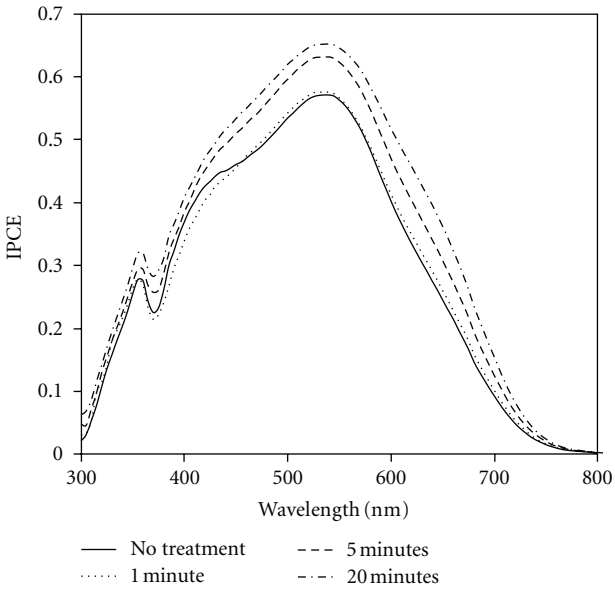

Figure 7: IPCE data for DSCs prepared from identical TiO_2 pastes treated with 2 M HNO_3 for differing times prior to sintering and dyeing under standard conditions.

reducing the dye uptake. The anion of the acid also appears to affect the performance of the cells, primarily by influencing the amount of dye uptake. Further work on the temporal evolution of film morphology in different acid exposure conditions must be performed to deconvolve the role of the anion from the kinetic effects of particle agglomeration.

Conflict of Interests

The authors do not have any conflict of interests with the content of the paper.

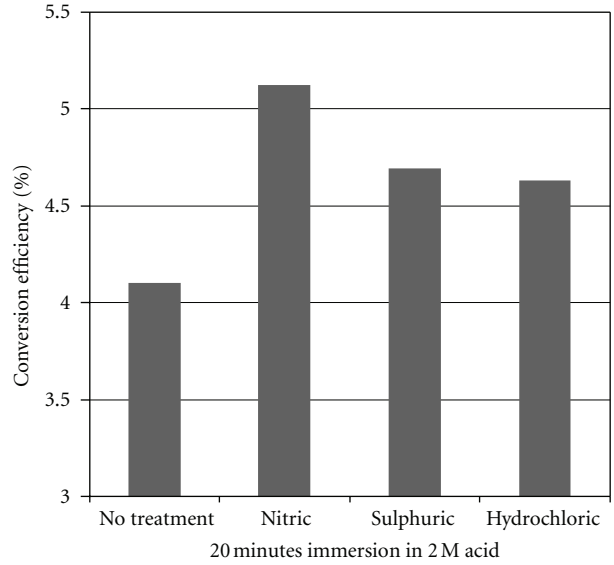

Figure 8: Influence of acid type (for a 20 minute immersion) on power conversion efficiency. H_3PO_4 is not shown due to its exceptionally poor performance.

Acknowledgments

The authors would like to thank the EPSRC and TSB for supporting this work through the SPECIFIC Innovation and Knowledge Centre. The authors would also like to gratefully acknowledge WAG and ERDF Low Carbon Research Institute (LCRI) convergence funding through the Solar Photovoltaic Academic Research Consortium (SPARC-Cymru).

References

[1] B. O'Regan and M. Grätzel, "A low-cost, high-efficiency solar cell based on dye-sensitized colloidal TiO_2 films," *Nature*, vol. 353, no. 6346, pp. 737–740, 1991.

[2] M. K. Nazeeruddin, A. Kay, I. Rodicio et al., "Conversion of light to electricity by cis-X_2bis(2,2′-bipyridyl-4,4′-dicarboxylate)ruthenium(II) charge-transfer sensitizers (X = Cl^-, Br^-, I^-, CN^-, and SCN^-) on nanocrystalline TiO_2 electrodes," *Journal of the American Chemical Society*, vol. 115, no. 14, pp. 6382–6390, 1993.

[3] M. Grätzel, "Photoelectrochemical cells," *Nature*, vol. 414, no. 6861, pp. 338–344, 2001.

[4] C. J. Barbé, F. Arendse, P. Comte et al., "Nanocrystalline titanium oxide electrodes for photovoltaic applications," *Journal of the American Ceramic Society*, vol. 80, pp. 3157–3171, 2005.

[5] K. Kalyanasundaram, S. Ito, S. Yanagida, and S. Uchida, "Scale-up and product development studies of dye-sensitized solar cells," in *Dye-Sensitized Solar Cells*, K. Kalyanasundaram, Ed., pp. 267–321, EPFL Press, Lausanne, Switzerland, 2010.

[6] T. Watson, I. Mabbett, H. Wang, L. Peter, and D. Worsley, "Ultrafast near infrared sintering of TiO_2 layers on metal substrates for dye-sensitized solar cells," *Progress in Photovoltaics: Research and Applications*, vol. 19, no. 4, pp. 482–486, 2011.

[7] M. Cherrington, T. C. Claypole, D. Deganello, I. Mabbett, T. Watson, and D. Worsley, "Ultrafast near-infrared sintering

of a slot-die coated nano-silver conducting ink," *Journal of Materials Chemistry*, vol. 21, pp. 7562–7564, 2011.

[8] P. J. Holliman, M. L. Davies, A. Connell, B. V. Velasco, and T. M. Watson, "Ultra-fast dye sensitisation and co-sensitisation for dye sensitized solar cells," *Chemical Communications*, vol. 46, no. 38, pp. 7256–7258, 2010.

[9] Y. Saito, S. Kambe, T. Kitamura, Y. Wada, and S. Yanagida, "Morphology control of mesoporous TiO_2 nanocrystalline films for performance of dye-sensitized solar cells," *Solar Energy Materials and Solar Cells*, vol. 83, no. 1, pp. 1–13, 2004.

[10] P. Sommeling, R. R. Haswell, H. J. P. Smit et al., "Influence of a $TiCl_4$ post-treatment on nanocrystalline TiO_2 films in dye-sensitized solar cells," *Society*, pp. 19191–19197, 2006.

[11] G. Rothenberger, M. Grätzel, and P. Comte, "A Contribution to the optical design of dye-sensitized nanocrystalline solar cells," *Solar Energy Materials and Solar Cells*, vol. 58, no. 3, pp. 321–336, 1999.

[12] J. Ferber and J. Luther, "Computer simulations of light scattering and absorption in dye-sensitized solar cells," *Solar Energy Materials and Solar Cells*, vol. 54, no. 1–4, pp. 265–275, 1998.

[13] K. Kalyanasundaram and M. Grätzel, "Applications of functionalized transition metal complexes in photonic and optoelectronic devices," *Coordination Chemistry Reviews*, vol. 177, pp. 347–414, 1998.

[14] Y. Tachibana, K. Hara, K. Sayama, and H. Arakawa, "Quantitative analysis of light-harvesting efficiency and electron-transfer yield in ruthenium-dye-sensitized nanocrystalline TiO_2 solar cells," *Chemistry of Materials*, vol. 14, no. 6, pp. 2527–2535, 2002.

[15] Z.-S. Wang, H. Kawauchi, T. Kashima, and H. Arakawa, "Significant influence of TiO_2 photoelectrode morphology on the energy conversion efficiency of N719 dye-sensitized solar cell," *Coordination Chemistry Reviews*, vol. 248, no. 13-14, pp. 1381–1389, 2004.

[16] A. Usami, "Theoretical study of application of multiple scattering of light to a dye-sensitized nanocrystalline photoelectrochemical cell," *Chemical Physics Letters*, vol. 277, no. 1–3, pp. 105–108, 1997.

[17] S. Hore, C. Vetter, R. Kern, H. Smit, and A. Hinsch, "Influence of scattering layers on efficiency of dye-sensitized solar cells," *Solar Energy Materials and Solar Cells*, vol. 90, no. 9, pp. 1176–1188, 2006.

[18] M. K. Nazeeruddin, R. Splivallo, P. Liska, P. Comte, and M. Grätzel, "A swift dye uptake procedure for dye sensitized solar cells," *Chemical Communications*, vol. 9, no. 12, pp. 1456–1457, 2003.

[19] P. Wang, S. M. Zakeeruddin, P. Comte, R. Charvet, R. Humphry-Baker, and M. Grätzel, "Enhance the performance of dye-sensitized solar cells by co-grafting amphiphilic sensitizer and hexadecylmalonic acid on TiO_2 nanocrystals," *Journal of Physical Chemistry B*, vol. 107, no. 51, pp. 14336–14341, 2003.

[20] Z.-S. Wang, F. Y. Li, and C. H. Huang, "Photocurrent enhancement of hemicyanine dyes containing RSO_3^- group through treating TiO_2 films with hydrochloric acid," *Journal of Physical Chemistry B*, pp. 9210–9217, 2001.

[21] Z.-S. Wang, T. Yamaguchi, H. Sugihara, and H. Arakawa, "Significant efficiency improvement of the black dye-sensitized solar cell through protonation of TiO_2 films," *Langmuir*, vol. 21, no. 10, pp. 4272–4276, 2005.

[22] H. S. Jung, J.-K. Lee, L. S. Lee, K. S. Hong, and H. Shin, "Acid adsorption on TiO_2 nanoparticles: an electrochemical properties study," *Journal of Physical Chemistry C*, vol. 112, no. 22, pp. 8476–8480, 2008.

[23] S. Hao, J. Wu, L. Fan, Y. Huang, J. Lin, and Y. Wei, "The influence of acid treatment of TiO_2 porous film electrode on photoelectric performance of dye-sensitized solar cell," *Solar Energy*, vol. 76, no. 6, pp. 745–750, 2004.

[24] T. M. Watson, P. Holliman, and D. Worsley, "Rapid, continuous in situ monitoring of dye sensitisation in dye-sensitized solar cells," *Journal of Materials Chemistry*, vol. 21, no. 12, pp. 4321–4325, 2011.

[25] M. Ikeda, N. Koide, L. Han, A. Sasahara, and H. Onishi, "Scanning tunneling microscopy study of black dye and deoxycholic acid adsorbed on a rutile $TiO_2(110)$," *Langmuir*, vol. 24, no. 15, pp. 8056–8060, 2008.